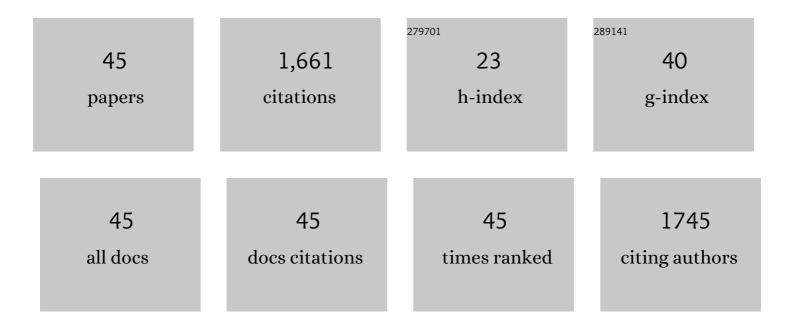
## Cheng-Jun Dong

List of Publications by Year in descending order

Source: https://exaly.com/author-pdf/8998711/publications.pdf Version: 2024-02-01



#	Article	IF	CITATIONS
1	Ru-functionalized Ni-doped dual phases of α/γ-Fe2O3 nanosheets for an optimized acetone detection. Journal of Nanostructure in Chemistry, 2023, 13, 577-589.	5.3	4
2	Enhanced microwave absorption of biomass carbon/nickel/polypyrrole (C/Ni/PPy) ternary composites through the synergistic effects. Journal of Alloys and Compounds, 2022, 890, 161887.	2.8	42
3	MOF-on-MOF nanoarchitecturing of Fe2O3@ZnFe2O4 radial-heterospindles towards multifaceted superiorities for acetone detection. Chemical Engineering Journal, 2022, 442, 136094.	6.6	31
4	Ternary MXene/MnO2/Ni composites for excellent electromagnetic absorption with tunable effective absorption bandwidth. Journal of Alloys and Compounds, 2022, 911, 165122.	2.8	12
5	Ni Doping in MnO <sub>2</sub> /MXene (Ti <sub>3</sub> C <sub>2</sub> T <sub><i>x</i></sub> ) Composites to Modulate the Oxygen Vacancies for Boosting Microwave Absorption. ACS Applied Electronic Materials, 2022, 4, 3694-3706.	2.0	13
6	Biomass derived porous carbon (BPC) and their composites as lightweight and efficient microwave absorption materials. Composites Part B: Engineering, 2021, 207, 108562.	5.9	177
7	Hierarchical flower-like NiFe2O4 with core–shell structure for excellent toluene detection. Rare Metals, 2021, 40, 1578-1587.	3.6	27
8	Gas sensing materials roadmap. Journal of Physics Condensed Matter, 2021, 33, 303001.	0.7	49
9	Interface engineering of N-doped Ni3S2/CoS2 heterostructures as efficient bifunctional catalysts for overall water splitting. Journal of Electroanalytical Chemistry, 2021, 895, 115516.	1.9	20
10	1D Zn2GeO4 rods supported on Ni foam for high performance non-enzymatic hydrogen peroxide sensor. Surfaces and Interfaces, 2021, 25, 101295.	1.5	3
11	A review on WO3 based gas sensors: Morphology control and enhanced sensing properties. Journal of Alloys and Compounds, 2020, 820, 153194.	2.8	200
12	NiO nanosheets on pine pollen-derived porous carbon: construction of interface to enhance microwave absorption. Journal of Materials Science: Materials in Electronics, 2020, , 1.	1.1	6
13	Synthesis of tin-glycerate and it conversion into SnO2 spheres for highly sensitive low-ppm-level acetone detection. Journal of Materials Science: Materials in Electronics, 2020, 31, 16539-16547.	1.1	15
14	ZnO-Decorated In/Ga Oxide Nanotubes Derived from Bimetallic In/Ga MOFs for Fast Acetone Detection with High Sensitivity and Selectivity. ACS Applied Materials & Interfaces, 2020, 12, 26161-26169.	4.0	54
15	In situ growth novel cubic copper hydroxyl phosphate and its utilization as a highly sensitive hydrogen peroxide amperometric sensor. Materials Today Communications, 2020, 24, 101212.	0.9	2
16	Soft-template synthesis of mesoporous NiFe2O4 for highly sensitive acetone detection. Journal of Materials Science: Materials in Electronics, 2020, 31, 6000-6007.	1.1	10
17	Tuning the microwave absorption capacity of TiP2O7 by composited with biomass carbon. Applied Surface Science, 2020, 515, 145974.	3.1	59
18	A nickel foam modified with electrodeposited cobalt and phosphor for amperometric determination of dopamine. Mikrochimica Acta, 2019, 186, 602.	2.5	6

CHENG-JUN DONG

#	Article	IF	CITATIONS
19	MOFs-Derived Porous NiFe2O4 Nano-Octahedrons with Hollow Interiors for an Excellent Toluene Gas Sensor. Nanomaterials, 2019, 9, 1059.	1.9	25
20	Jute-based porous biomass carbon composited by Fe3O4 nanoparticles as an excellent microwave absorber. Journal of Alloys and Compounds, 2019, 803, 1119-1126.	2.8	51
21	Highly Sensitive and Selective Toluene Sensor of Bimetallic Ni/Fe-MOFs Derived Porous NiFe <sub>2</sub> O <sub>4</sub> Nanorods. Industrial & Engineering Chemistry Research, 2019, 58, 9450-9457.	1.8	27
22	In situ fabrication of Ni(OH)2 nanoflakes/K-Ti-O nanowires on NiTi foil for high performance non-enzymatic hydrogen peroxide sensing. Journal of Electroanalytical Chemistry, 2019, 842, 107-114.	1.9	5
23	Biomass carbon derived from pine nut shells decorated with NiO nanoflakes for enhanced microwave absorption properties. RSC Advances, 2019, 9, 9126-9135.	1.7	73
24	Preparation and electromagnetic shielding effectiveness of cobalt ferrite nanoparticles/carbon nanotubes composites. Nanomaterials and Nanotechnology, 2019, 9, 184798041983782.	1.2	26
25	Nanoparticles Assembled CdIn2O4 Spheres with High Sensing Properties towards n-Butanol. Nanomaterials, 2019, 9, 1714.	1.9	17
26	In situ fabrication of Co(OH)2 by hydrothermal treating Co foil in MOH (M = H, Li, Na, K) for non-enzymatic glucose detection. Journal of Alloys and Compounds, 2019, 781, 1033-1039.	2.8	11
27	MOFs-derived NiFe2O4 fusiformis with highly selective response to xylene. Journal of Alloys and Compounds, 2019, 784, 102-110.	2.8	40
28	Microwave absorption performance of Ni(OH)2 decorating biomass carbon composites from Jackfruit peel. Applied Surface Science, 2018, 447, 261-268.	3.1	89
29	SnO2 quantum dots with rapid butane detection at lower ppm-level. Applied Physics A: Materials Science and Processing, 2018, 124, 1.	1.1	4
30	Synthesis of core-shell carbon sphere@nickel oxide composites and their application for supercapacitors. Ionics, 2018, 24, 513-521.	1.2	19
31	Nonaqueous synthesis of Pd-functionalized SnO2/In2O3 nanocomposites for excellent butane sensing properties. Sensors and Actuators B: Chemical, 2018, 257, 419-426.	4.0	21
32	Direct growth of MnCO3 on Ni foil for a highly sensitive nonenzymatic glucose sensor. Journal of Alloys and Compounds, 2018, 762, 216-221.	2.8	14
33	Cu <sub>2</sub> O templating strategy for the synthesis of octahedral Cu <sub>2</sub> O@Mn(OH) <sub>2</sub> core–shell hierarchical structures with a superior performance supercapacitor. Journal of Materials Chemistry A, 2018, 6, 13668-13675.	5.2	56
34	Carbon spheres@MnO2 core-shell nanocomposites with enhanced dielectric properties for electromagnetic shielding. Scientific Reports, 2017, 7, 15841.	1.6	38
35	Combustion synthesized hierarchically porous Mn <sub>3</sub> O <sub>4</sub> for catalytic degradation of methyl orange. Canadian Journal of Chemical Engineering, 2017, 95, 643-647.	0.9	6
36	Monodisperse ZnFe 2 O 4 nanospheres synthesized by a nonaqueous route for a highly slective low-ppm-level toluene gas sensor. Sensors and Actuators B: Chemical, 2017, 239, 1231-1236.	4.0	50

CHENG-JUN DONG

#	Article	IF	CITATIONS
37	Facile synthesis of core–shell carbon nanotubes@MnOOH nanocomposites with remarkable dielectric loss and electromagnetic shielding properties. RSC Advances, 2016, 6, 90002-90009.	1.7	20
38	Self-grown MnO 2 nanosheets on carbon fiber paper as high-performance supercapacitors electrodes. Electrochimica Acta, 2016, 217, 16-23.	2.6	43
39	Binder-free NiO@MnO 2 core-shell electrode: Rod-like NiO core prepared through corrosion by oxalic acid and enhanced pseudocapacitance with sphere-like MnO 2 shell. Electrochimica Acta, 2016, 189, 83-92.	2.6	47
40	Facile synthesis of CuO micro-sheets over Cu foil in oxalic acid solution and their sensing properties towards n-butanol. Journal of Materials Chemistry C, 2016, 4, 985-990.	2.7	14
41	Surfactant-mediated synthesis of ZnCo2O4 powders as a high-performance anode material for Li-ion batteries. lonics, 2015, 21, 623-628.	1.2	9
42	Butane detection: W-doped TiO <sub>2</sub> nanoparticles for a butane gas sensor with high sensitivity and fast response/recovery. RSC Advances, 2015, 5, 96539-96546.	1.7	26
43	Porous NiO nanosheets self-grown on alumina tube using a novel flash synthesis and their gas sensing properties. RSC Advances, 2015, 5, 4880-4885.	1.7	52
44	Combustion synthesis of porous Pt-functionalized SnO <sub>2</sub> sheets for isopropanol gas detection with a significant enhancement in response. Journal of Materials Chemistry A, 2014, 2, 20089-20095.	5.2	106
45	Hydrothermal growth of ZnO nanorods on Zn substrates and their application in degradation of azo dyes under ambient conditions. CrystEngComm, 2014, 16, 7761-7770.	1.3	42